journal

J. Am. Ceram. Soc., **97** [8] 2646–2653 (2014)
DOI: 10.1111/jace.12987

Crystal Structure and Elastic Properties of Hypothesized MAX Phase-Like Compound $(Cr_2Hf)_2Al_3C_3$

Yuxiang Mo,† Sitaram Aryal, Paul Rulis, and Wai-Yim Ching*

Department of Physics and Astronomy, University of Missouri-Kansas City, Kansas City, Missouri 64110

The term "MAX phase" refers to a very interesting and important class of layered ternary transition-metal carbides and nitrides with a novel combination of both metal and ceramic-like properties that have made these materials highly regarded candidates for numerous technological and engineering applications. Using $(Cr_2Hf)_2Al_3C_3$ as an example, we demonstrate the possibility of incorporating more types of elements into a MAX phase while maintaining the crystallinity, instead of creating solid solution phases. The crystal structure and elastic properties of MAX phase-like $(Cr_2Hf)_2Al_3C_3$ are studied using the Vienna *ab initio* Simulation Package. Unlike MAX phases with a hexagonal symmetry ($P6_3/mmc$, #194), $(Cr_2Hf)_2Al_3C_3$ crystallizes in the monoclinic space group of $P2_1/m$ (#11) with lattice parameters of a = 5.1739 Å, b = 5.1974 Å, c = 12.8019 Å; $\alpha = \beta = 90°$, $\gamma = 119.8509°$. Its structure is found to be energetically much more favorable with an energy (per formula unit) of −102.11 eV, significantly lower than those of the allotropic segregation (−100.05 eV) and solid solution (−100.13 eV) phases. Calculations using a stress versus strain approach and the VRH approximation for polycrystals also show that $(Cr_2Hf)_2Al_3C_3$ has outstanding elastic moduli.

I. Introduction

The material under study, $(Cr_2Hf)_2Al_3C_3$, is derived from Cr_2AlC which belongs to a large family of novel compounds: layered ternary transition-metal carbides and nitrides. The early discoveries[1–7] of these compounds (in powder form) date back to the 1960s. Three decades later, using a reactive hot-pressing method, Barsoum and El-Raghy[8] successfully fabricated single-phase Ti_3SiC_2 in polycrystalline bulk form, which enabled the observation of its unusual mechanical and transport properties. Such a development drew new attention to these carbides and nitrides, which have been extensively studied ever since.[9–15] The chemical compositions for most of these compounds can be summarized by a general formula: $M_{n+1}AX_n$ [M: an early transition-metal element, A: an A group (III, IV, V, or VI) element, X: carbon or nitrogen, and n = 1–6], which is the reason why these compounds are also known as "MAX phases". In a MAX phase, hexagonal near close-packed M, A, and X atoms form layered structures. Figure 1(a) shows the unit cell of Cr_2AlC, which is sometimes called a "(2 1 1)" phase because the stoichiometric ratio of the constituent elements is 2:1:1. MAX phases involve a combination of metallic, covalent, and ionic bonds[16] among the composing atoms. Very recently, we made available[17] quantitative bond order values for the various species of bonds in MAX phases using Mulliken analysis. This uncommon blend of bonding types in MAX phases has given these nanolaminated materials a very intricate and intriguing combination of both metal and ceramic-like properties. They are good conductors of heat and electricity. They are lightweight, stiff, and refractory, but also easily machinable. They can tolerate external damages and internal defects, as well as thermal shocks and high-temperature oxidation. Ongoing and prospective applications of this remarkable group of materials include cutting tools,[18] saws, brazed tools, nozzles, bearings, rotating parts in disk drives,[10] tools for die pressing, biocompatible materials,[11] electrodes, rotating electrical contacts,[13] resistors, capacitors, heat exchangers,[10] heating elements, kiln furniture, porous exhaust filter for automobiles, vacuum tube coatings in solar hot water systems, jet-engine components,[19] coating materials on blades of gas/steam turbines, nuclear applications,[20,21] projectile-proof armor, fuselage materials of spacecraft to block infrared[22] and shield the craft from micrometeoroids and orbital debris, etc.

In addition to phases of the conventional $M_{n+1}AX_n$ formula, MAX phases with alternative stoichiometry and stacking sequence[23–25] have also been discovered. Other new materials in relation to MAX phases include ternary perovskite borides[26] and nitrides[27] (space group of $Pm\bar{3}m$, $CaTiO_3$ as the prototype), Al_3BC_3[28] (a metal borocarbide containing linear C–B–C units), orthorhombic Mo_2BC[29] (space group of *Cmcm*), the newly discovered MXene[30] (2D nanosheets created via exfoliation of MAX phase), and so on. It has also been of genuine interest to investigate both experimentally (examples[31–42]) and theoretically[43–48] how adding more types of elements into a MAX phase would alter (and allow the tuning of) its properties, largely because the novel MAX phase itself was originally derived from conventional ceramics (binary transition-metal carbides and nitrides) by adding A group elements into them. Using $(Cr_2Hf)_2Al_3C_3$ as an example, we demonstrate, starting from a crystallographic point of view, the possibility of incorporating more types of elements into a MAX phase while maintaining the crystallinity, instead of creating solid solution phases. Such preservation of crystallinity could not only provide exotic mechanical properties (as shown later) but also preserve tribological advantages[49,50] and high electrical and thermal conductivities (due to the ease of electron and phonon scattering through periodic lattices). Compared with the solid solution, a crystalline phase with a lower coefficient of friction can have a critical advantage in friction-reduction, self-lubrication, and wear-resistant applications. With a higher electrical conductivity, it can have better performance and less energy dissipation in electrical applications. And with a higher thermal conductivity, it can better protect itself (by efficient elimination of temperature gradients) against thermal shocks in high-temperature structural applications.

II. Crystal Structure

In this work, the combination of Cr and Hf was used to study novel changes of properties because these two elements

Y. Zhou—contributing editor

Manuscript No. 33992. Received October 28, 2013; approved April 11, 2014.
*Fellow, The American Ceramic Society.
†Author to whom correspondence should be addressed. e-mail: yuxiangm@gmail.com

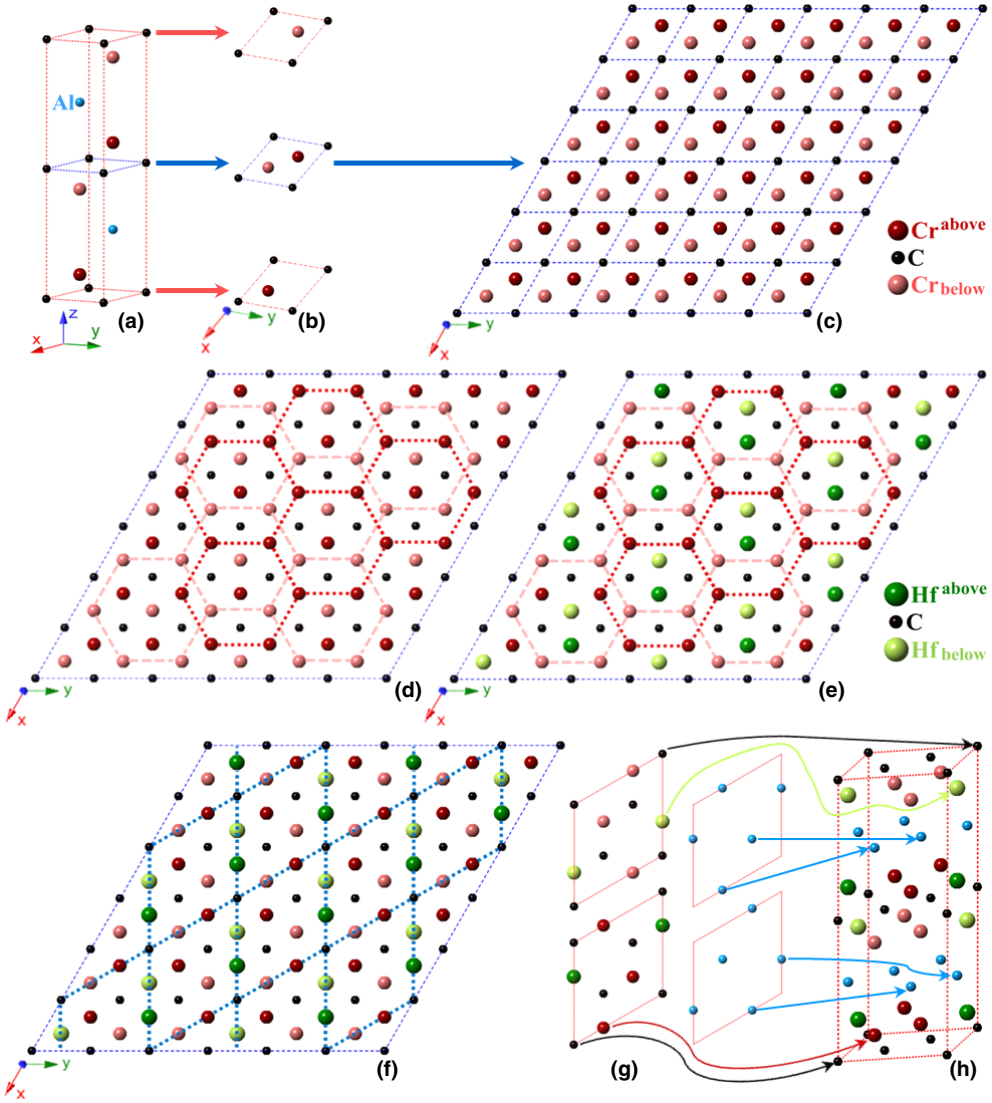

Fig. 1. The crystallographic evolution from Cr_2AlC to $(Cr_2Hf)_2Al_3C_3$. (a) The unit cell of Cr_2AlC. (b) Cr–C layers separated from (a). (c) A 6×6 expansion of the middle layer in (b). (d) The same structure as that of (c), but with hexagons facilitating the observation of the hexagonal arrangements. (e) The structure from (c), with the central Cr atom in each hexagon replaced by Hf. (f) The same structure as that of (e), but with blue frames indicating the new unit cell. Derived in a similar approach from the top and bottom layers of (b), the left column of (g) shows the other two new layers, and the right column of (g) shows the new Al layers. (h) shows the preliminary unit cell of $(Cr_2Hf)_2Al_3C_3$, assembled with all the cell layers from (g) and (f).

have a large contrast of atomic radii and numbers of valence electrons. In practice, many other elements could be adopted for the combination, forming a large series (detailed later) of potential new materials. Figure 1 delineates how the crystal structure of $(Cr_2Hf)_2Al_3C_3$ is developed from that of Cr_2AlC. The central idea is the replacement of Cr atoms at the center of each hexagon with another type of atoms (Hf, in the present case). This is illustrated schematically by the replacement of Fig. 1(d) with Fig. 1(e). Stoichiometry-wise, each hexagon in Fig. 1(e) uniquely includes 1 Hf atom at its center, while leaving 6 Cr atoms at the six vertices. However, each of these Cr atoms is simultaneously shared by another two adjacent hexagons. So for each hexagon, there are $6 \times \frac{1}{1+2} = 2$ Cr atoms. The ratio for Cr and Hf in the crystal is 2:1, hence the chemical formula $(Cr_2Hf)_2Al_3C_3$.

To relax the crystal structure of $(Cr_2Hf)_2Al_3C_3$, we used the Vienna *ab initio* Simulation Package (VASP),[51–53] with the implementation of the projector augmented wave (PAW) approach and the Perdew–Burke–Ernzerhof (PBE) exchange-correlation functional. An energy cutoff of 600 eV was set for the PAW-PBE potential and a Monkhorst Γ-centered $7 \times 7 \times 3$ k-point mesh was used. The Methfessel–Paxton scheme was employed for the smearing of the Fermi surface. The electronic and ionic-force iterations converged to the level of 10^{-6} eV and 10^{-4} eV/Å, respectively. Detailed in Fig. 2 is the VASP-relaxed crystal structure of $(Cr_2Hf)_2Al_3C_3$. Comparing it with the initial model in Figs. 1(f)–(h), the Hf atoms have deviated from the Cr planes and formed new sublayers, mainly due to their larger atomic radii. Such extrusion of Hf atoms caused the shifting of Al atoms. An example is the Al atom ($x = 0.1598$, $y = 0.4908$, $z = 0.75$) in layer "2" of Fig. 2, which was originally located at the $x = 0$ cell boundary. The overall crystal lattice is also distorted by the atomic size difference. Constants for the new lattice are: $a = 5.1739$ Å, $b = 5.1974$ Å, $c = 12.8019$ Å; $\alpha = \beta = 90°$, $\gamma = 119.8509°$.

It is also noticeable from the γ angle in Fig. 2 that unlike the predecessor, MAX phase, $(Cr_2Hf)_2Al_3C_3$ does not belong to the hexagonal symmetry group anymore. Figure 3 is a plot of the crystal structures with extra colored lines that help illustrate the symmetry group for $(Cr_2Hf)_2Al_3C_3$. In Fig. 3(a), only when the lattice is rotated by 180° (so that the blue pseudorhombus revolves to overlap with the magenta pseudorhombus) could the rotated lattice overlap with the original lattice after a $c/2$ translation in the z direction. Any smaller rotation (to the yellow rhombus or green

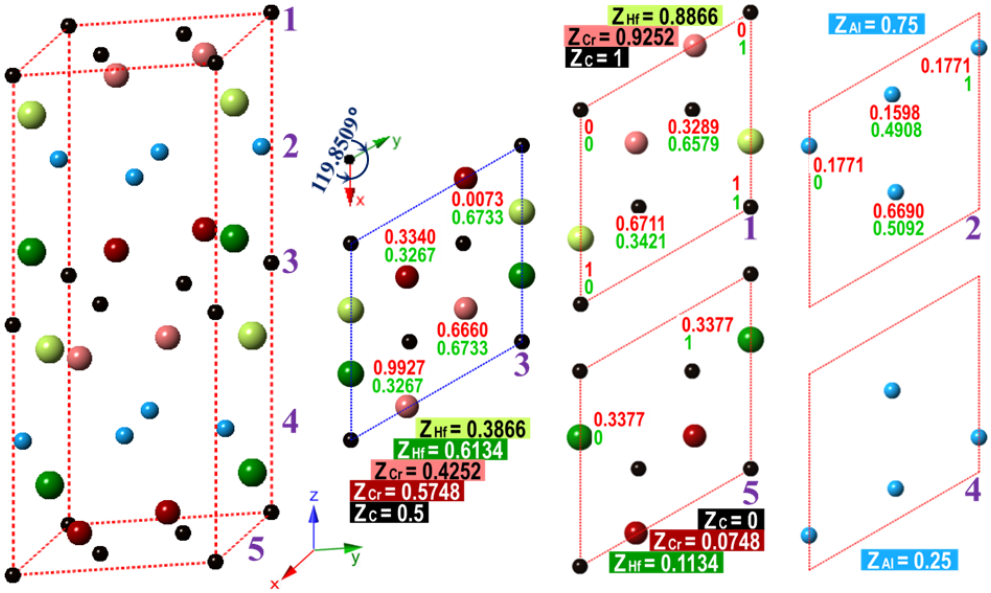

Fig. 2. The relaxed crystal structure of $(Cr_2Hf)_2Al_3C_3$. Shown on the left is the unit cell of $(Cr_2Hf)_2Al_3C_3$ with purple numbers "1", "2", "3", "4", and "5" to its right, marking different layers. And shown on the right are the views of the five layers in the direction from $+z$ to $-z$. Color strips contain the z parameters for each type of atoms. And numbers in red (upper) and green (lower) are the fractional x and y coordinates for individual atoms. Atoms without coordinates listed can be easily positioned according to symmetry.

pseudorhombus) would not be able to achieve the overlap after translations, because such rotations would move Hf atoms to the locations originally possessed by Cr atoms. So far it can be determined that the primitive cell has a twofold (360°/180°) screw axis with a translation of 1/2 of the c lattice vector. In the Hermann–Mauguin notation, this is denoted by "$P2_1$". To find possible mirror planes and glide planes for $(Cr_2Hf)_2Al_3C_3$, a look first at Cr_2AlC (the progenitor) would be very helpful. In Fig. 3(b), there are two mirror planes: the vertical plane in green (crossing C, Al, and Cr) and the horizontal plane in blue (crossing only Al). The crystal structure stays unchanged after reflections of every atom according to either of the mirror planes. Here, the unit cell of Cr_2AlC is chosen to have the Al atom at the $z = 0$ cell boundary, for the purpose of showing the symmetry associated with the horizontal mirror plane. Figure 3(c) shows the glide plane in purple. Reflections of every atom according to this plane result in a structure that needs a $c/2$ translation in the z direction before it can overlap with the original structure. The two mirror planes and one glide plane shown in Figs. 3(b) and (c) are represented by "*mmc*" in $P6_3/mmc$, the Hermann–Mauguin notation for the space group of Cr_2AlC. From the unit cell of $(Cr_2Hf)_2Al_3C_3$ (which also has Al atoms at its $z = 0$ cell boundary) in Fig. 3(d), it can be observed that the reflection invariance for the horizontal mirror plane still holds, but that for the vertical mirror plane does not exist anymore. Returning back to Fig. 3(a), the thin dotted line in green which crosses four C atoms indicates the hypothetical vertical mirror plane. It is apparent that Hf and Cr atoms are not mirror images of each other. Meanwhile, a is not equal to b, so they would not be a pair of mirror images either even if they were the same type of atoms. A similar reasoning can easily tell that the hypothetical glide plane denoted by the thin dotted line in purple is not appropriate either. What remains in the case of $(Cr_2Hf)_2Al_3C_3$ is only one horizontal mirror plane. And this leads us finally to the complete Hermann–Mauguin notation: $P2_1/m$ (#11, in the monoclinic space group). With the relaxed structure of $(Cr_2Hf)_2Al_3C_3$, we used the PowderCell program[54] to simulate its X-ray (CuK_α = 1.540598 Å) diffraction pattern, which is plotted in Fig. 4. Such information provides a reference for future experimental confirmations of the phase. The electronic density of states is also calculated for $(Cr_2Hf)_2Al_3C_3$, using the first-principles orthogonalized linear combination of atomic orbitals (OLCAO) method.[55] The total energy was evaluated on a $7 \times 7 \times 3$ k-point mesh in the irreducible portion of the Brillouin zone, and brought to convergence (0.0001 a.u. limit) in 81 iterations. Plotted in Fig. 5 is the electronic density of states for $(Cr_2Hf)_2Al_3C_3$. Like a MAX phase, this material is still metallic. Its total density of states (TDOS) at the Fermi level (E_f) is 18.65 states/(eV·cell). This fairly large value is primarily due to the relatively large number of atoms (24) in the unit cell. The major contributor to the TDOS at E_f are the Cr-3d states [13.23 states/(eV·cell)], which can be attributed to the abundance of 3d electrons (5 per Cr atom) and the large number of Cr atoms (8 per unit cell).

III. Total Energies and Elastic Properties

The energy convergence during the structural relaxation and the adequate stress under small strains (detailed in the next paragraph) suggest that the crystal structure of $(Cr_2Hf)_2Al_3C_3$ is at an energy minimum (structurally stable). This is the only condition always required for the ability of a material to exist. A structure does not necessarily have to possess the lowest energy among all the allotropic phases to be able to exist, otherwise there would not be any allotropes for any given chemical composition. In material systems that have relatively low energy barriers between different allotropic phases and less flexible methods (and conditions) of preparation and heat treatment. it is possible for the energy comparison to influence the purity and mass availability of a certain phase. To find out whether and to what extent $(Cr_2Hf)_2Al_3C_3$ is energetically favorable against its possible competing phases (that have the same chemical composition), additional VASP calculations of total energies were performed on six structures: a $(Cr_2Hf)_2Al_3C_3$ $1 \times 1 \times 3$ supercell versus a segregation model, a $(Cr_2Hf)_2Al_3C_3$ $3 \times 3 \times 1$ supercell versus a solid solution model, Cr_2AlC unit cell, and Hf_2AlC unit cell. The structures of the first two sets of models are shown in Figs. 6 and 7, respectively. Listed in Table I are the numerical parameters and results of the calculations. Per formula unit, $(Cr_2Hf)_2Al_3C_3$ has an energy of −102.11 eV, significantly lower than those of the segregation (−100.05 eV), solid solution (−100.13 eV), and 2 (Cr_2AlC) + Hf_2AlC mixture (−101.04 eV). These energy differences of 1.07–2.06 eV per formula unit are quite large,

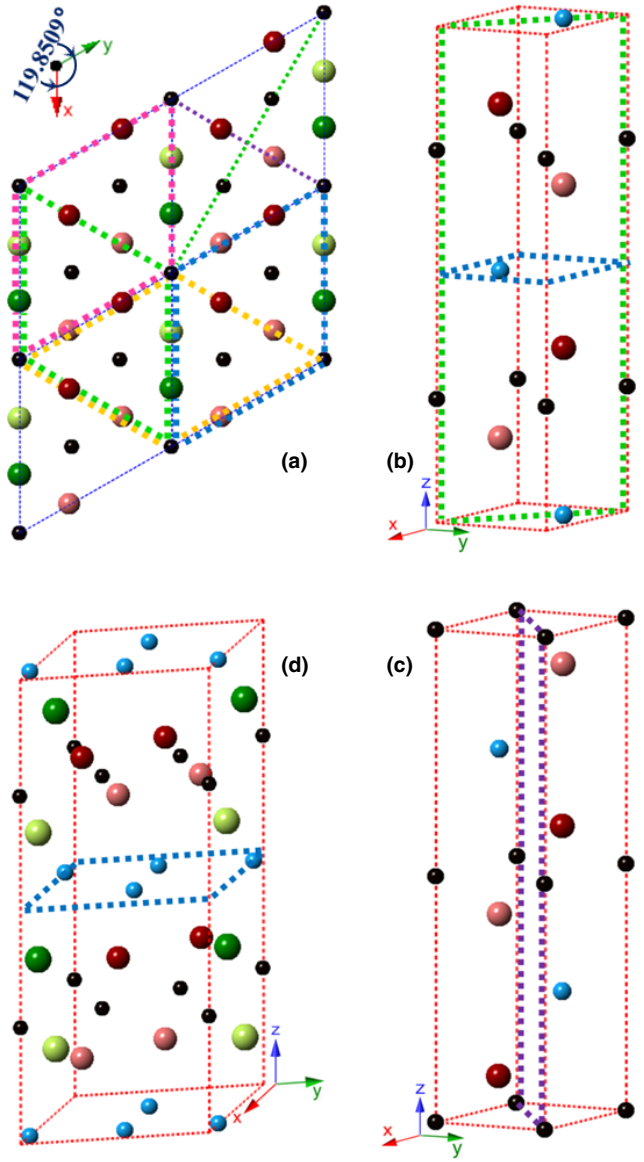

Fig. 3. The space group symmetry of $(Cr_2Hf)_2Al_3C_3$. (a) The view (in the direction from $+z$ to $-z$) of a $2 \times 2 \times 1$ supercell of $(Cr_2Hf)_2Al_3C_3$. (b) The unit cell of Cr_2AlC, with two mirror planes in green and blue. (c) The unit cell of Cr_2AlC, with one glide plane in purple. (d) The unit cell of $(Cr_2Hf)_2Al_3C_3$, with one mirror plane in blue.

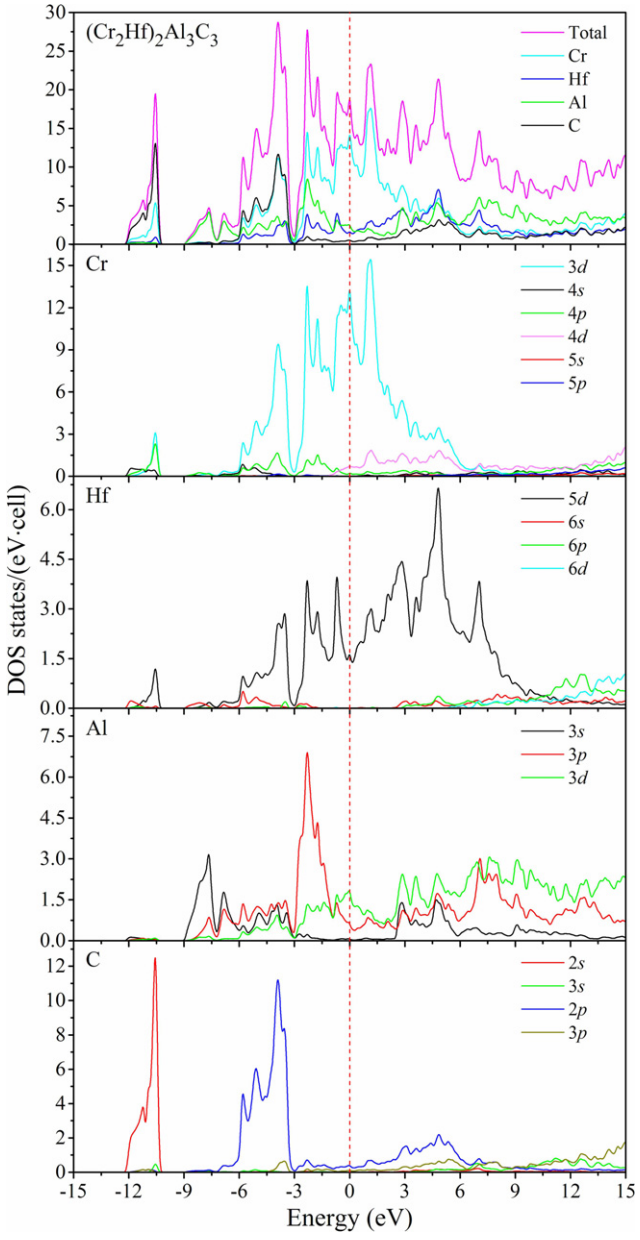

Fig. 5. The electronic density of states for $(Cr_2Hf)_2Al_3C_3$. Total and atom-resolved DOS are shown on top, followed underneath by orbital-resolved DOS of each composing element.

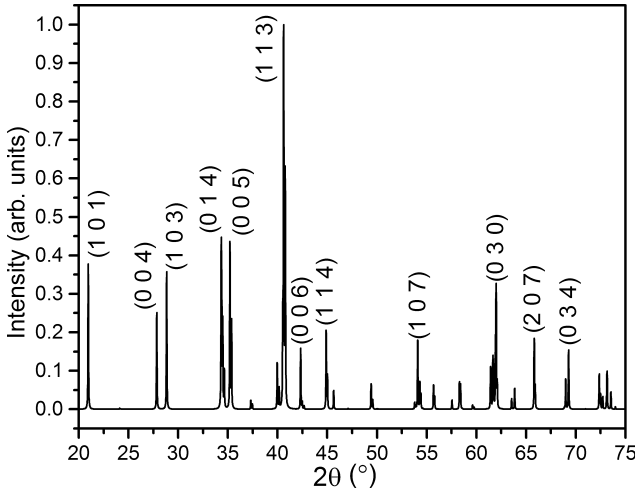

Fig. 4. Indexed X-ray diffraction pattern of $(Cr_2Hf)_2Al_3C_3$

equivalent to 103–199 kJ/mol. This indicates that the crystalline $(Cr_2Hf)_2Al_3C_3$ is much more preferable than the segregation, solid solution, and $2(Cr_2AlC) + Hf_2AlC$ mixture, because large inputs of net energy are needed for Hf atoms in $(Cr_2Hf)_2Al_3C_3$ to form pure layers (segregation), break the order in Cr layers (forming solid solution), or even for $(Cr_2Hf)_2Al_3C_3$ to completely degrade to Cr_2AlC and Hf_2AlC. Meanwhile, $(Cr_2Hf)_2Al_3C_3$ is calculated to have a density of 7.58 g/cm^3, 4.26%–6.76% higher than those of the segregation (7.25 g/cm^3), solid solution (7.10 g/cm^3), and 2 $(Cr_2AlC) + Hf_2AlC$ mixture (7.27 g/cm^3). Therefore, $(Cr_2Hf)_2Al_3C_3$ is suggested to be resistant to not only temperature but also pressure-induced phase transitions.

To further compare the crystalline $(Cr_2Hf)_2Al_3C_3$ with the segregation and solid solution in the mechanical perspective, the intrinsic elastic properties have also been calculated according to the strain–stress analysis scheme by Nielsen and Martin.[56] For each of these three phases and Hf_2AlC, a small compression (−1%) and expansion (+1%) were applied to each fully relaxed strain element. This compression/expan-

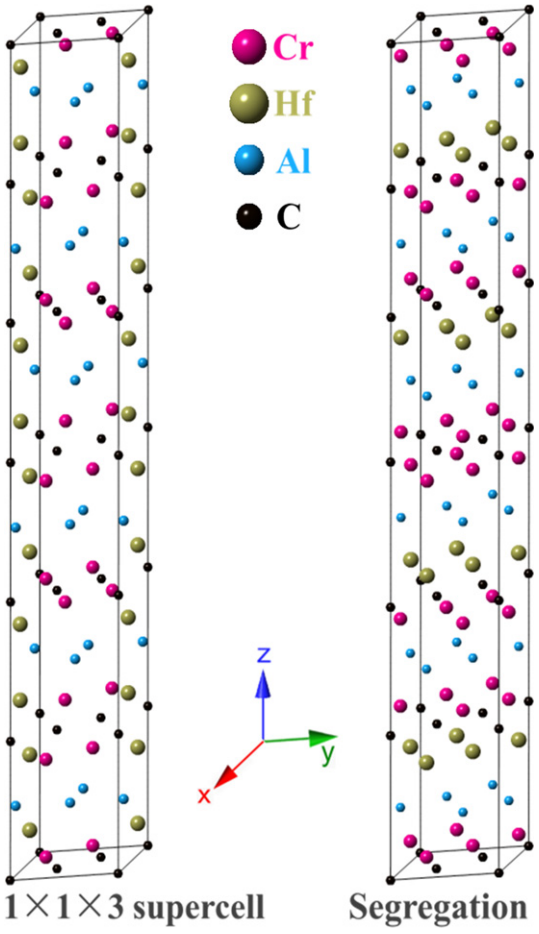

Fig. 6. Crystal structures of the relaxed $(Cr_2Hf)_2Al_3C_3$ 1 × 1 × 3 supercell and segregation. The purpose of using a supercell is to include enough Hf atoms for the composition of an integer number of pure Hf layers in the segregation model.

sion rate was chosen as an optimal balance between linear elastic response and numerical accuracy. Keeping the volume and shape of these strained cells fixed, the atomic positions were fully relaxed again with the same computational configurations as those in Table I (for the segregation, solid solution, and Hf_2AlC) and Section II [for the unit-cell $(Cr_2Hf)_2Al_3C_3$]. The resultant stress tensor (σ_i) ($i = xx$, yy, zz, yz, zx, xy) was used in combination with each corresponding strain (ε_j) to calculate the elastic tensor elements C_{ij}, according to the system of linear equations:

$$\sigma_{ij}=\sum_{ij} C_{ij}\varepsilon_j \tag{1}$$

Using the Voigt–Reuss–Hill approximation,[57–59] the bulk mechanical parameters were then calculated from the elastic (C_{ij}) and compliance (S_{ij}) tensor elements. The Voigt approximation gives the upper limit for the parameters:

$$K_V = \frac{1}{9}(C_{11} + C_{22} + C_{33}) + \frac{2}{9}(C_{12} + C_{13} + C_{23}) \tag{2}$$

$$G_V = \frac{1}{15}(C_{11} + C_{22} + C_{33} - C_{12} - C_{13} - C_{23}) + \frac{1}{5}(C_{44} + C_{55} + C_{66}) \tag{3}$$

And the Reuss approximation gives the lower limit for the parameters:

$$K_R = \frac{1}{(S_{11} + S_{22} + S_{33}) + 2(S_{12} + S_{13} + S_{23})} \tag{4}$$

$$G_R = \frac{15}{4(S_{11}+S_{22}+S_{33}) - 4(S_{12}+S_{13}+S_{23}) + 3(S_{44}+S_{55}+S_{66})} \tag{5}$$

The Hill approximation as the average of the above two limits has been proven to be a good characterization of polycrystalline bulk properties of a variety of pristine[60–63] and defect-containing materials.[64–69] The average of the two bounds is given by the following set of equations:

$$K = (K_V + K_R)/2, \quad G = (G_V + G_R)/2,$$
$$E = 9KG/(3K + G), \text{and } \eta = (3K - 2G)/2(3K + G) \tag{6}$$

Listed in Table II are the elastic coefficients, bulk moduli (K), shear moduli (G), Young's moduli (E), Poisson's ratio (η), and G/K ratio for the five phases. In terms of bulk moduli, Crystalline $(Cr_2Hf)_2Al_3C_3$ is elastically much stiffer than the allotropic segregation and solid solution phases, as it has larger elastic moduli across the board: a bulk modulus of 181.5 GPa which is 19.6% and 21.9% larger than those of the segregation and solid solution, a shear modulus of 125.2 GPa which is 19.5% and 40.7% larger than those of the segregation and solid solution, and a Young's modulus of 305.3 GPa which is 19.4% and 37.1% larger than those of the segregation and solid solution. To put these in the whole picture, in the drastic decline of elastic stiffness during the transit from Cr_2AlC to Hf_2AlC, the segregation already has its elastic moduli almost comparable to those of Hf_2AlC. The solid solution even has smaller shear and Young's moduli than those of Hf_2AlC. Yet stoichiometrically the segregation and solid solution only have one-third of the Cr atoms replaced with Hf atoms. However, in sharp contrast, crystalline $(Cr_2Hf)_2Al_3C_3$ retains over 90% of the elastic stiffness of Cr_2AlC. As for the Poisson's ratio, most of these five phases fall in a fairly narrow range from 0.200 to 0.220 which is typical for MAX phases, whereas the solid solution has a relatively higher (but still in line) Poisson's ratio of 0.251. The Pugh ratio (G/K) for crystalline $(Cr_2Hf)_2Al_3C_3$ and the segregation phase are both 0.69, smaller than those of the Cr_2AlC (0.73) and Hf_2AlC (0.75). While the solid solution phase has the smallest Pugh ratio of 0.60 which equals the k_{crit} value[70] established for a fairly large group of MAX phases, indicating that the solid solution phase is the least brittle among the five phases in this study, but it is in the middle compared with other MAX phases.

There are various transition-metal elements available to play the roles of Cr and Hf in crystalline $(Cr_2Hf)_2Al_3C_3$. And the replacement of the central atom in each hexagon is not restricted to the M site only. The same pattern could be achieved at the A or X site. In addition, this type of phase does not have to be based on a (2 1 1) MAX phase. It could also come from (3 1 2) and (4 1 3) phases. Therefore, the general formula should be $(M1_2M2)_{n+1}(A1_2A2)(X1_2X2)_n$. Here "M1" and "M2" denote transition-metal elements. When M1 ≠ M2, their stoichiometric ratio is 2:1, just like the case for Cr and Hf in $(Cr_2Hf)_2Al_3C_3$; When M1 = M2, there is no replacement of M1 (in other words, the M site is pure). Exactly the same usage works as well for A1, A2, and X1, X2. And "n" represents the number of stacking layers. These proposed new crystals may inherit a significant portion of wonderful properties from MAX phases, but in the sense of crystallography they represent a new group of materials.

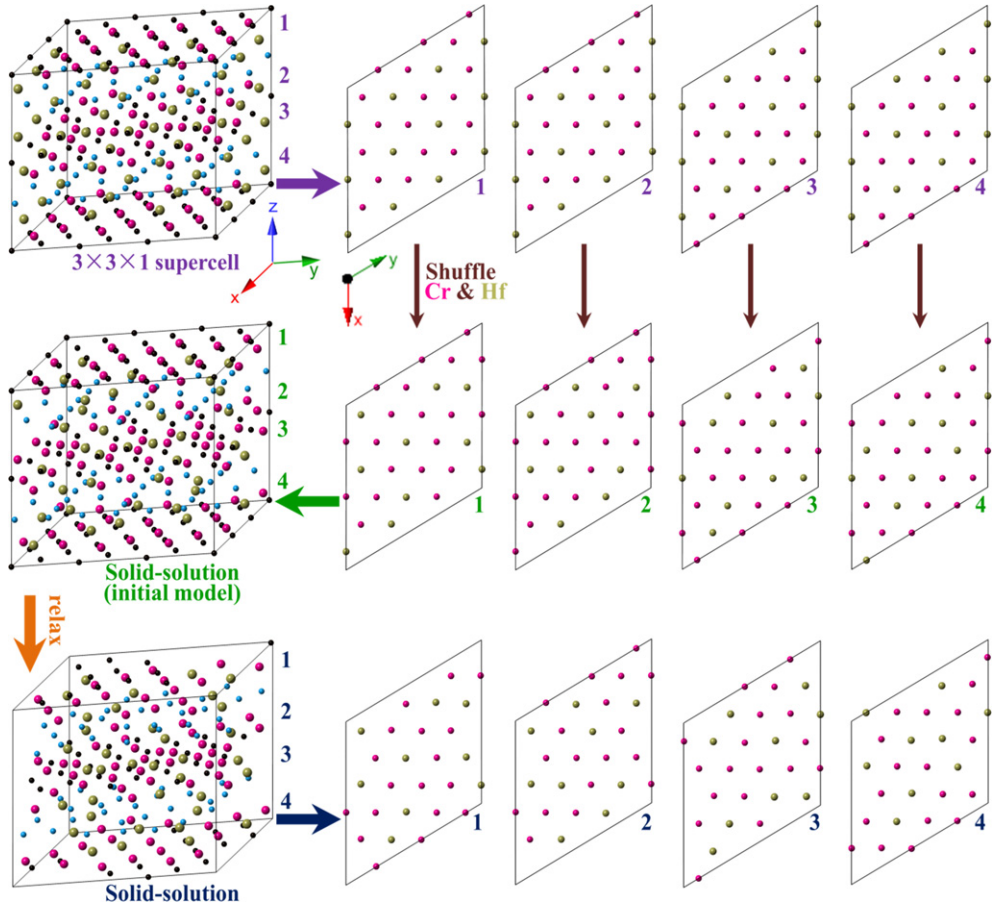

Fig. 7. The construction of the solid-solution model based on the $(Cr_2Hf)_2Al_3C_3$ 3 × 3 × 1 supercell. The threefold duplications in the *x* and *y* directions of a unit cell enable the shuffling of the Cr and Hf atoms.

Table I. Computational Configurations and Results for the $(Cr_2Hf)_2Al_3C_3$ Supercells, Segregation, Solid Solution, Cr_2AlC, and Hf_2AlC

	1 × 1 × 3 supercell	Segregation	3 × 3 × 1 supercell	Solid solution	Cr_2AlC	Hf_2AlC
Number of atoms	72	72	216	216	8	8
k-point mesh	5 × 5 × 1	5 × 5 × 1	1 × 1 × 1	1 × 1 × 1	15 × 15 × 3	15 × 15 × 3
Convergence						
Electronic (eV)	10^{-6}	10^{-6}	10^{-6}	10^{-6}	10^{-6}	10^{-6}
Ionic force (eV/Å)	10^{-4}	10^{-4}	10^{-4}	10^{-4}	10^{-4}	10^{-4}
Total energy (eV)						
Per cell	−612.79	−600.29	−1837.49	−1802.26	−65.32	−71.43
Per formula unit	−102.13	−100.05	−102.08	−100.13	−101.04	
Lattice constants						
a (Å)	5.17	5.21	15.56	15.75	2.85	3.27
b (Å)	5.20	5.21	15.61	15.74	2.85	3.27
c (Å)	38.41	39.88	12.79	13.38	12.69	14.39
α (°)	90.00	90.00	90.00	90.07	90.00	90.00
β (°)	90.00	90.00	90.00	90.15	90.00	90.00
γ (°)	119.86	120.00	119.90	119.99	120.00	120.00
Volume ($Å^3$)	895.55	937.50	2693.14	2872.91	89.27	133.26
Density (g/cm^3)	7.59	7.25	7.57	7.10	7.27	

Table II. The Elastic Coefficients and Intrinsic Mechanical Properties (in GPa) of Cr_2AlC, $(Cr_2Hf)_2Al_3C_3$ (unit cell), Segregation, Solid Solution, and Hf_2AlC

	C_{11}	C_{33}	C_{44}	C_{66}	C_{12}	C_{13}	K	G	E	η	G/K
Cr_2AlC[70]	364.5	356.1	139.8	140.0	84.4	107.4	187.0	136.1	328.6	0.207	0.73
$(Cr_2Hf)_2Al_3C_3$	355.2	333.6	120.1	136.6	80.9	107.4	181.5	125.2	305.3	0.220	0.69
Segregation	280.5	295.9	112.7	108.3	64.6	99.4	151.8	104.8	255.7	0.219	0.69
Solid-solution	286.3	237.6	86.6	102.4	77.3	94.2	148.9	89.0	222.7	0.251	0.60
Hf_2AlC	295.4	262.0	103.5	112.9	69.6	71.6	141.8	106.5	255.5	0.200	0.75

We call them "D-MAX" phases because they can have "double" elements at one site. Although D-MAX phases currently await being experimentally synthesized and characterized, it is possible to surmise some general trends in their mechanical characteristics with respect to the structural and elemental variations. Enlarging the stacking number (n) of a D-MAX phase would make it behave more like a ceramic because of the increased stoichiometric content of the ceramic component. Replacing a transition-metal element (be it M1 or M2) with another transition-metal element of a comparable size but a larger number of valence electrons could strengthen the hybrid bonds and thereby stiffen the D-MAX phase. But replacing a transition-metal element (either M1 or M2) with another transition-metal element of the same number of valence electrons (isoelectronic) but a larger size would enlarge the bond lengths and weaken the D-MAX phase. Enlarging the difference in the atomic sizes of the two transition-metal elements (the larger atom being M2) could enlarge the energy differences between the D-MAX phase and its allotropes, provided that the numbers of valence electrons are kept the same for each element. The same trends should also apply to the A site. And for the X site, the introduction of N would strengthen the original phase.

IV. Summary and Conclusions

We have studied the crystal structure and elastic properties of $(Cr_2Hf)_2Al_3C_3$ which is an example of a new type of MAX-like crystalline phases. It is found to be energetically much more preferable than competing segregation, solid solution, and precursor structures. It also has outstanding elastic properties compared with the segregation and solid solution phases, preserving over 90% of the elastic stiffness of Cr_2AlC despite a 33.3% substitution of Cr by Hf atoms. According to the formula of D-MAX phases, and the possible MAX-phase elements[71] (M1, M2 = Sc, Ti, Zr, Hf, V, Nb, Ta, Cr, and Mo; A1, A2 = Cd, Al, Ga, In, Tl, Si, Ge, Sn, Pb, P, As, and S; X1, X2 = C and N; n = 1–6) from the periodic table, a mathematical permutation and combination analysis suggests that there are 278640 potential D-MAX phases. Obviously, only a small portion of them could actually be synthesized. In the case of their progenitor, MAX phases, a similar analysis would predict that there can be 1296 phases, but so far the number of successfully[14] synthesized MAX phases is well below 100. Nevertheless, the variety of present MAX phases has already fascinated many researchers and new phases continue being discovered. We hope our work encourages others to not only experimentally synthesize members of the proposed D-MAX species via powder metallurgy and vapor deposition methods, but also theoretically predict which D-MAX phases, among the vast many, are more likely to be synthesized in pure samples by comparing the energy with that of the associated segregation, solid solution, and precursor phases.

Acknowledgments

This work was supported by the US Department of Energy (DOE), National Energy Technology Laboratory under grant no. DE-FE0005865. This research used the resources of the National Energy Research Scientific Computing Center supported by the Office of Science of DOE under contract no. DE-AC03-76SF00098.

References

[1]W. Jeitschko, H. Nowotny, and F. Benesovsky, "Carbon-Containing Ternary Compounds (H-Phase)," *Monatsh. Chem.*, **94** [4] 672–6 (1963).

[2]W. Jeitschko, H. Nowotny, and F. Benesovsky, "The H-Phases Ti_2InC, Zr_2InC, Hf_2InC, and Ti_2GeC," *Monatsh. Chem.*, **94** [6] 1201–5 (1963).

[3]D. I. Bardos and P. A. Beck, "Electron Phases in Certain Ternary Alloys of Transition Metals with Silicon," *Trans. Metall. Soc. AIME*, **236** [1] 64–9 (1966).

[4]W. Jeitschko and H. Nowotny, "Crystal Structure of Ti_3SiC_2, a New Type of Complex Carbide," *Monatsh. Chem.*, **98** [2] 329–37 (1967).

[5]H. Wolfsgruber, H. Nowotny, and F. Benesovsky, "Crystal Structure of Titanium Germanium Carbide (Ti_3GeC_2)," *Monatsh. Chem.*, **98** [6] 2403–5 (1967).

[6]H. Nowotny and F. Benesovsky, "Crystal Structures of Transition Metal Carbides and Nitrides," *Planseeberichte Fuer Pulvermetallurgie*, **16** [3] 204–14 (1968).

[7]O. Beckmann, H. Boller, H. Nowotny, and F. Benesovsky, "Complex Carbides and Nitrides in the Systems Ti-(Zn, Cd, Hg)-(C, N) and Cr-Ga-N," *Monatsh. Chem.*, **100** [5] 1465–70 (1969).

[8]M. W. Barsoum and T. El-Raghy, "Synthesis and Characterization of a Remarkable Ceramic: Ti_3SiC_2," *J. Am. Ceram. Soc.*, **79** [7] 1953–6 (1996).

[9]Z. Lin, M. Li, and Y. Zhou, "TEM Investigations on Layered Ternary Ceramics," *J. Mater. Sci. Technol.*, **23** [2] 145–65 (2007).

[10]M. W. Barsoum, "The $M_{N+1}AX_N$ Phases: A New Class of Solids; Thermodynamically Stable Nanolaminates," *Prog. Solid State Chem.*, **28** [1–4] 201–81 (2000).

[11]J. Wang and Y. Zhou, "Recent Progress in Theoretical Prediction, Preparation, and Characterization of Layered Ternary Transition-Metal Carbides," *Annu. Rev. Mater. Res.*, **39**, 415–43 (2009).

[12]X. H. Wang and Y. Zhou, "Layered Machinable and Electrically Conductive Ti_2AlC and Ti_3AlC_2 Ceramics: A Review," *J. Mater. Sci. Technol.*, **26** [5] 385–416 (2010).

[13]P. Eklund, M. Beckers, U. Jansson, H. Hoegberg, and L. Hultman, "The $M_{n+1}AX_n$ Phases: Materials Science and Thin-Film Processing," *Thin Solid Films*, **518** [8] 1851–78 (2010).

[14]Z. M. Sun, "Progress in Research and Development on MAX Phases: A Family of Layered Ternary Compounds," *Int. Mater. Rev.*, **56** [3] 143–66 (2011).

[15]M. W. Barsoum and M. Radovic, "Elastic and Mechanical Properties of the MAX Phases," *Annu. Rev. Mater. Res.*, **41**, 195–227 (2011).

[16]X. Wang and Y. Zhou, "Solid-Liquid Reaction Synthesis and Simultaneous Densification of Polycrystalline Ti_2AlC," *Z. Metallkd.*, **93** [1] 66–71 (2002).

[17]Y. Mo, P. Rulis, and W. Y. Ching, "Electronic Structure and Optical Conductivities of 20 MAX-Phase Compounds," *Phys. Rev. B*, **86**, 165122, 10pp (2012).

[18]L. Pierre de Rochemont, "Cutting Tool and Method of Manufacture"; US Patent 20120012403A1, 2012.

[19]Q. M. Wang, A. Flores Renteria, O. Schroeter, R. Mykhaylonka, C. Leyens, W. Garkas, and M. to Baben, "Fabrication and Oxidation Behavior of Cr_2AlC Coating on Ti6242 Alloy," *Surf. Coat. Technol.*, **204** [15] 2343–52 (2010).

[20]J. C. Nappé, Ph. Grosseau, F. Audubert, B. Guilhot, M. Beauvy, M. Benabdesselam, and I. Monnet, "Damages Induced by Heavy Ions in Titanium Silicon Carbide: Effects of Nuclear and Electronic Interactions at Room Temperature," *J. Nucl. Mater.*, **385** [2] 304–7 (2009).

[21]F. Meng, L. Chaffron, and Y. Zhou, "Synthesis of Ti_3SiC_2 by High Energy Ball Milling and Reactive Sintering from Ti, Si, and C Elements," *J. Nucl. Mater.*, **386–388**, 647–9 (2009).

[22]S. Li, R. Ahuja, M. W. Barsoum, P. Jena, and B. Johansson, "Optical Properties of Ti_3SiC_2 and Ti_4AlN_3," *Appl. Phys. Lett.*, **92**, 221907, 3pp (2008).

[23]J.-P. Palmquist, S. Li, P. O. Å. Persson, J. Emmerlich, O. Wilhelmsson, H. Högberg, M. I. Katsnelson, B. Johansson, R. Ahuja, O. Eriksson, L. Hultman, and U. Jansson, "$M_{n+1}AX_n$ Phases in the Ti-Si-C System Studied by Thin-Film Synthesis and *ab Initio* Calculations," *Phys. Rev. B*, **70**, 165401, 13pp (2004).

[24]H. Högberg, P. Eklund, J. Emmerlich, J. Birch, and L. Hultman, "Epitaxial Ti_2GeC, Ti_3GeC_2, and Ti_4GeC_3 MAX-Phase Thin Films Grown by Magnetron Sputtering," *J. Mater. Res.*, **20** [04] 779–82 (2005).

[25]X. Wang, H. Zhang, L. Zheng, Y. Ma, X. Lu, Y. Sun, and Y. Zhou, "$Ti_5Al_2C_3$: A New Ternary Carbide Belonging to MAX Phases in the Ti-Al-C System," *J. Am. Ceram. Soc.*, **95** [5] 1508–10 (2012).

[26]D. Music, Z. Sun, and J. M. Schneider, "Alternating Covalent-Ionic and Metallic Bonding in Perovskite Borides Studied Using *ab Initio* Methods," *Phys. Rev. B*, **71**, 052104, 3pp (2005).

[27]D. Music and J. M. Schneider, "Elastic Properties of MFe_3N (M = Ni, Pd, Pt) Studied by *ab Initio* Calculations," *Appl. Phys. Lett.*, **88**, 031914, 3pp (2006).

[28]J. Wang, Y. Zhou, T. Liao, and Z. Lin, "First-Principles Prediction of Low Shear-Strain Resistance of Al_3BC_3: A Metal Borocarbide Containing Short Linear BC_2 Units," *Appl. Phys. Lett.*, **89**, 021917, 3pp (2006).

[29]J. Emmerlich, D. Music, M. Braun, P. Fayek, F. Munnik, and J. M. Schneider, "A Proposal for an Unusually Stiff and Moderately Ductile Hard Coating Material: Mo_2BC," *J. Phys. D: Appl. Phys.*, **42**, 185406, 6pp (2009).

[30]M. Naguib, M. Kurtoglu, V. Presser, J. Lu, J. Niu, M. Heon, L. Hultman, Y. Gogotsi, and M. W. Barsoum, "Two-Dimensional Nanocrystals Produced by Exfoliation of Ti_3AlC_2," *Adv. Mater.*, **23** [37] 4248–53 (2011).

[31]H. Nowotny, P. Rogl, and J. C. Schuster, "Structural Chemistry of Complex Carbides and Related Compounds," *J. Solid State Chem.*, **44** [1] 126–33 (1982).

[32]M. A. Pietzka and J. C. Schuster, "Phase Equilibria in the Quaternary System Ti-Al-C-N," *J. Am. Ceram. Soc.*, **79** [9] 2321–30 (1996).

[33]M. W. Barsoum, T. El-Raghy, and M. Ali, "Processing and Characterization of Ti_2AlC, Ti_2AlN, and $Ti_2AlC_{0.5}N_{0.5}$," *Metall. Mater. Trans. A*, **31** [7] 1857–65 (2000).

[34]S. Gupta and M. W. Barsoum, "Synthesis and Oxidation of V_2AlC and $(Ti_{0.5},V_{0.5})_2AlC$ in Air," *J. Electrochem. Soc.*, **151** [2] D24–9 (2004).

[35]F. Meng, Y. Zhou, and J. Wang, "Strengthening of Ti_2AlC by Substituting Ti with V," *Scripta Mater.*, **53** [12] 1369–72 (2005).
[36]M. Radovic, M. W. Barsoum, A. Ganguly, T. Zhen, P. Finkel, S. R. Kalidindi, and E. Lara-Curzio, "On the Elastic Properties and Mechanical Damping of Ti_3SiC_2, Ti_3GeC_2, $Ti_3Si_{0.5}Al_{0.5}C_2$ and Ti_2AlC in the 300-1573 K Temperature Range," *Acta Mater.*, **54** [10] 2757–67 (2006).
[37]O. Wilhelmsson, J.-P. Palmquist, E. Lewin, J. Emmerlich, P. Eklund, P. O. Å. Persson, H. Högberg, S. Li, R. Ahuja, O. Eriksson, L. Hultman, and U. Jansson, "Deposition and Characterization of Ternary Thin Films Within the Ti-Al-C System by DC Magnetron Sputtering," *J. Cryst. Growth*, **291** [1] 290–300 (2006).
[38]H. Yang, B. Manoun, R. T. Downs, A. Ganguly, and M. W. Barsoum, "Crystal Chemistry of Layered Carbide, $Ti_3(Si_{0.43}Ge_{0.57})C_2$," *J. Phys. Chem. Solids*, **67** [12] 2512–6 (2006).
[39]A. Ganguly, M. W. Barsoum, and R. D. Doherty, "Interdiffusion Between Ti_3SiC_2-Ti_3GeC_2 and Ti_2AlC-Nb_2AlC Diffusion Couples," *J. Am. Ceram. Soc.*, **90** [7] 2200–4 (2007).
[40]B. Manoun, S. K. Saxena, G. Hug, A. Ganguly, E. N. Hoffman, and M. W. Barsoum, "Synthesis and Compressibility of $Ti_3(Al,Sn_{0.2})C_2$ and $Ti_3Al(C_{0.5},N_{0.5})_2$," *J. Appl. Phys.*, **101**, 113523, 7pp (2007).
[41]J. Rosen, P. O. Å. Persson, M. Ionescu, A. Kondyurin, D. R. McKenzie, and M. M. M. Bilek, "Oxygen Incorporation in Ti_2AlC Thin Films," *Appl. Phys. Lett.*, **92**, 064102, 3pp (2008).
[42]P. O. Å. Persson, J. Rosen, D. R. McKenzie, and M. M. M. Bilek, "Formation of the MAX-Phase Oxycarbide $Ti_2AlC_{1-x}O_x$ Studied Via Electron Energy-Loss Spectroscopy and First-Principles Calculations," *Phys. Rev. B*, **80**, 092102, 4pp (2009).
[43]N. I. Medvedeva, D. L. Novikov, A. L. Ivanovsky, M. V. Kuznetsov, and A. J. Freeman, "Electronic Properties of Ti_3SiC_2-Based Solid Solutions," *Phys. Rev. B*, **58**, 16042–50 (1998).
[44]J. Wang and Y. Zhou, "First-Principles Study of Equilibrium Properties and Electronic Structure of $Ti_3Si_{0.75}Al_{0.25}C_2$ Solid Solution," *J. Phys.: Condens. Matter*, **15** [35] 5959–68 (2003).
[45]Z. Sun, R. Ahuja, and J. M. Schneider, "Theoretical Investigation of the Solubility in $(M_xM'_{2-x})AlC$ (M and M′=Ti,V,Cr)," *Phys. Rev. B*, **68**, 224112, 4pp (2003).
[46]J. Wang and Y. Zhou, "*Ab Initio* Elastic Stiffness of Nano-Laminate $(M_xM'_{2-x})$ AlC (M and M′ = Ti, V and Cr) Solid Solution," *J. Phys.: Condens. Matter*, **16** [16] 2819–27 (2004).
[47]P. Finkel, B. Seaman, K. Harrell, J. Palma, J. D. Hettinger, S. E. Lofland, A. Ganguly, M. W. Barsoum, Z. Sun, S. Li, and R. Ahuja, "Electronic, Thermal, and Elastic Properties of $Ti_3Si_{1-x}Ge_xC_2$ Solid Solutions," *Phys. Rev. B*, **70**, 085104, 6pp (2004).
[48]Y. L. Du, Z. M. Sun, H. Hashimoto, and M. W. Barsoum, "Theoretical Investigations on the Elastic and Thermodynamic Properties of $Ti_2AlC_{0.5}N_{0.5}$ Solid Solution," *Phys. Lett. A*, **374** [1] 78–82 (2009).
[49]S. Myhra, J. W. B. Summers, and E. H. Kisi, "Ti_3SiC_2–A Layered Ceramic Exhibiting Ultra-Low Friction," *Mater. Lett.*, **39** [1] 6–11 (1999).
[50]A. Crossley, E. H. Kisi, J. W. B. Summers, and S. Myhra, "Ultra-Low Friction for a Layered Carbide-Derived Ceramic, Ti_3SiC_2, Investigated by Lateral Force Microscopy (LFM)," *J. Phys. D: Appl. Phys.*, **32** [6] 632–8 (1999).
[51]G. Kresse and J. Hafner, "*Ab Initio* Molecular Dynamics for Liquid Metals," *Phys. Rev. B*, **47** [1] 558–61 (1993).
[52]G. Kresse and J. Furthmüller, "Efficiency of *ab-Initio* Total Energy Calculations for Metals and Semiconductors Using a Plane-Wave Basis Set," *Comput. Mater. Sci.*, **6** [1] 15–50 (1996).
[53]G. Kresse and J. Furthmüller, "Efficient Iterative Schemes for *ab Initio* Total-Energy Calculations Using a Plane-Wave Basis Set," *Phys. Rev. B*, **54** [16] 11169–86 (1996).
[54]G. Nolze and W. Kraus, PowderCell. http://www.ccp14.ac.uk/ccp/web-mirrors/powdcell/a_v/v_1/powder/e_cell.html, 1998.
[55]W. Y. Ching and P. Rulis, *Electronic Structure Methods for Complex Materials: The Orthogonalized Linear Combination of Atomic Orbitals*. Oxford University Press, oxford, 2012.
[56]O. H. Nielsen and R. M. Martin, "First-Principles Calculation of Stress," *Phys. Rev. Lett.*, **50** [9] 697–700 (1983).
[57]W. Voigt, *Handbook of Crystal Physics*. Taubner, Leipzig, 1928.
[58]A. Reuss, "Calculation of the Yield Strength of Mixed Crystals Due to the Plasticity Condition for Single Crystals," *Zeitschrift für Angewandte Mathematik und Mechanik*, **9** [1] 49–58 (1929).
[59]R. Hill, "The Elastic Behavior of a Crystalline Aggregate," *Proc. Phys. Soc. A*, **65** [5] 349–54 (1952).
[60]H. Yao, L. Ouyang, and W. Y. Ching, "*Ab Initio* Calculation of Elastic Constants of Ceramic Crystals," *J. Am. Ceram. Soc.*, **90** [10] 3194–204 (2007).
[61]W. Y. Ching, S. Aryal, P. Rulis, and W. Schnick, "Electronic Structure and Physical Properties of the Spinel-Type Phase of BeP_2N_4 From All-Electron Density Functional Calculations," *Phys. Rev. B*, **83**, 155109, 8pp (2011).
[62]W. Y. Ching, L. Ouyang, P. Rulis, and H. Yao, "*Ab Initio* Study of the Physical Properties of γ-Al_2O_3: Lattice Dynamics, Bulk Properties, Electronic Structure, Bonding, Optical Properties, and ELNES/XANES Spectra," *Phys. Rev. B*, **78**, 014106, 13pp (2008).
[63]S. Aryal, P. Rulis, and W. Y. Ching, "Mechanical Properties and Electronic Structure of Mullite Phases Using First-Principles Modeling," *J. Am. Ceram. Soc.*, **95** [7] 2075–88 (2012).
[64]W. Y. Ching, P. Rulis, L. Ouyang, and A. Misra, "*Ab Initio* Tensile Experiment on a Model of an Intergranular Glassy Film in β-Si_3N_4 with Prismatic Surfaces," *Appl. Phys. Lett.*, **94**, 051907, 3pp (2009).
[65]W. Y. Ching, P. Rulis, and A. Misra, "*Ab Initio* Elastic Properties and Tensile Strength of Crystalline Hydroxyapatite," *Acta Biomater.*, **5** [8] 3067–75 (2009).
[66]L. Liang, P. Rulis, and W. Y. Ching, "Mechanical Properties, Electronic Structure and Bonding of α- and β-Tricalcium Phosphates with Surface Characterization," *Acta Biomater.*, **6** [9] 3763–71 (2010).
[67]S. Aryal, P. Rulis, and W. Y. Ching, "Mechanism for Amorphization of Boron Carbide B_4C Under Uniaxial Compression," *Phys. Rev. B*, **84**, 184112, 12pp (2011).
[68]W. Y. Ching, P. Rulis, L. Ouyang, S. Aryal, and A. Misra, "Theoretical Study of the Elasticity, Mechanical Behavior, Electronic Structure, Interatomic Bonding, and Dielectric Function of an Intergranular Glassy Film Model in Prismatic β-Si_3N_4," *Phys. Rev. B*, **81**, 214120, 14pp (2010).
[69]S. Aryal, P. Rulis, L. Ouyang, and W. Y. Ching, "Structure and Properties of the Low-Density Phase ι-Al_2O_3 from First Principles," *Phys. Rev. B*, **84**, 174123, 12pp (2011).
[70]W. Y. Ching, Y. Mo, S. Aryal, and P. Rulis, "Intrinsic Mechanical Properties of 20 MAX-Phase Compounds," *J. Am. Ceram. Soc.*, **96** [7] 2292–7 (2013).
[71]M. W. Barsoum and T. El-Raghy, "The MAX Phases: Unique New Carbide and Nitride Materials," *Am. Sci.*, **89** [4] 334–43 (2001). □